IEEE Access
Multidisciplinary | Rapid Review | Open Access Journal

Received 17 March 2023, accepted 9 April 2023, date of publication 12 April 2023, date of current version 24 April 2023.

Digital Object Identifier 10.1109/ACCESS.2023.3266723

APPLIED RESEARCH

Voltage Stability of Spacecraft Electric Power Systems for Deep Space Exploration

MARC A. CARBONE[1], (Member, IEEE), AMIRHOSSEIN SAJADI[2], (Senior Member, IEEE), JORDAN M. MURRAY[3], JEFFREY T. CSANK[1], AND KENNETH A. LOPARO[3], (Life Fellow, IEEE)

[1]Power Management and Distribution Branch, NASA Glenn Research Center, Cleveland, OH 44135, USA
[2]Renewable and Sustainable Energy Institute (RASEI), University of Colorado Boulder, Boulder, CO 80309, USA
[3]Department of Electrical, Computer and Systems Engineering, Institute for Smart, Secure and Connected Systems (ISSACS), Case Western Reserve University, Cleveland, OH 44106, USA

Corresponding author: Marc A. Carbone (marc.a.carbone@nasa.gov)

This work was supported by the NASA's Exploration Systems Development Mission Directorate/Exploration Capabilities.

ABSTRACT The future of deep space exploration requires high levels of reliability in critical subsystems such as the electrical power system. This paper provides an analysis of voltage stability of direct current (DC) microgrids for spacecraft applications. Bifurcation theory is used to determine the behavior of the system and identify the major causes of voltage instability. The analytical results of the bifurcation model are experimentally verified through a series of tests emulating probable operating conditions of the spacecraft. The findings of this paper are applicable to similar classes of islanded (grid forming) DC electric power systems including aerospace vehicles, shipboard systems, and terrestrial microgrids.

INDEX TERMS Autonomous power system, bifurcation, DC microgrid, spacecraft, voltage stability.

I. INTRODUCTION

Electric power systems in space applications have evolved with a particular emphasis on the use of independent power systems (commonly referred to as islanded microgrids), such as the power system on board the International Space Station (ISS) [1]. This class of electric power systems is defined by a group of interconnected generation sources and loads that have the capability to operate independently or interconnected with another power system [2]. This paper specifically studies microgrids on board modern spacecraft currently under development with application to future deep space exploration.

Microgrids are designed to safely ride through disturbances and serve the connected load and to reconfigure and disconnect a subset of loads when necessary, for example during a period of stress on the system, and then reconnect the load when possible and desired [3], [4], [5], [6]. Spacecraft applications like the ISS typically function as grid forming (islanded) microgrids but require occasional docking events from visiting vehicles that mirrors a similar process to those for interconnection and coordination (transition from grid forming to grid following) in terrestrial microgrids.

Microgrids on board modern spacecraft are typically DC. This design offers merits that suit the application to extraterrestrial electric power systems and has several advantages over alternating current (AC) systems for lunar power system applications [7], [8]. First, they provide *higher efficiency* given DC generation sources such as solar photovoltaics (PV), fuel cells, and battery storage units that are efficiently integrated in a DC system with fewer conversions. Second, they offer *reduced complexity* for control and operation given that functions such as frequency regulation, synchronization, and reactive power control are not necessary. Third, they offer *higher reliability* due to the limited number of power electronic converters and inverters that are necessary for these systems.

Presently, critical supervision for spacecraft including the management of the DC microgrid on board the vehicle travelling within the low earth orbit (LEO) is achieved by human operators that are managing operations from ground stations on earth. However, in order to advance the human understanding of this universe and for human exploration of space and interplanetary habitation, deep space travels are necessary.

The associate editor coordinating the review of this manuscript and approving it for publication was Zhenbao Liu.

In fact, the National Aeronautics and Space Administration (NASA)'s current focus centers on developing high power vehicles to travel into deep space. A key challenge for developing these vehicles is the management, reliability, and resilience of the microgrid on board the spacecraft as it will play a critical role in the success of space missions. Communication delays for missions beyond the LEO are estimated to be significant (e.g. as much as 44 minutes round trip for Mars missions [9]). Due to the potential dangers of these communication delays, many of the monitoring functions currently conducted by ground personnel must be done by autonomous software systems on board the spacecraft that are capable of intelligent decision-making. The capability to operate autonomously would allow the spacecraft to intelligently and dynamically operate under varying operating conditions with minimal external assistance or human intervention.

To achieve autonomy, the key is to develop an understanding of the dynamics and behavior of the system states as the basis for independent decision-making by the control agents when subjected to external events (e.g. disturbances or faults in the system) or changes in the operating environment [10]. The control and management of DC microgrids is concerned with voltage stability as a function of power regulation where distribution feeders are purely resistive [11]. Thus, to achieve autonomy within the context of DC microgrids, it is reasonable to focus attention on the voltage dynamics and stability so that this knowledge can be used for the development of the independent decision-making processes that are required to robustly govern the system under a wide range of operating conditions.

Extensive research and experimentation on the operation and management of terrestrial DC microgrids including the problem of voltage stability have been reported in the literature. See [12] for a review of stability and control in different microgrid architectures considering only terrestrial applications. The literature suggests that voltage stability has also been studied for several spacecraft electric power system designs, a few of which are discussed below. The concept of energy management for extraterrestrial DC electric systems has been discussed in [13] and [14]. In [15], feedforward terms are added to a V-I based droop controller to guarantee exponential stability in terrestrial DC-DC converters. Reference [16] analyzes the stability of DC microgrids with hybrid (battery and supercapacitor) energy storage systems. The stability of DC power electronics utilizing nonlinear droop control is studied in [17]. A stability assessment for a zonal ship DC microgrid is provided in [18] by eigenvalue analysis. Several methods for understanding power system stability and security have been established using artificial intelligence (AI) and machine learning (ML) approaches. See [19] for a review. These techniques, however, are not suitable for autonomous spacecraft applications at this time. Reasons for this include, (1) the lack of verification and validation (V&V) processes for these methods, and (2) the limited computational resources for such algorithms on a space flight computer. Currently there exists a gap in the understanding of stability and autonomous control of modern space-based DC microgrids with specific applications to high- powered, highly distributed spacecraft which this paper aims to bridge.

The contributions of this paper are threefold. First, it provides an experimentally validated theoretical model for DC microgrids found on board modern spacecraft for deep space travel applications including solar PV generation, energy storage, and constant power loads, with a particular emphasis on distributed energy storage. Second, this paper establishes necessary conditions and parametric sensitivity for the stability of a DC space electric power system and unveils the instability mechanism under varying operating conditions that are derived from design considerations and strenuously harsh ambient modern spacecraft have to operate in. Third, it provides experimental hardware testing on the explicit observation of subcritical Hopf bifurcation phenomenon. Even though we report this novel observation for DC microgrids onboard spacecraft, it advances the field of microgrid stability overall, by expanding upon recent research efforts including [20], where bifurcation analysis is used to study terrestrial microgrids, but lacked sufficient hardware experimentation to support the theory. Similarly, [21] uses a more detailed Lyapunov-based model to analyze DC microgrid stability, which is not suitable to be used for a real-time algorithm on a radiation hardened flight computer.

To this end, first, we develop an approximate state space model of the spacecraft electrical distribution system and then analyze this network to understand the dynamics of this class of power system. Individual subsystem models developed in [20], [22], and [23] are used to construct this analytical model for the electrical power distribution network. The complete model is built by interconnecting approximate models of PV arrays, parallel batteries, and various types of loads. We discuss and explain specific design consideration and operational challenges associated with this class of power system are discussed to identify edge cases that present most concern. These edge cases then are studied by applying the bifurcation theory to the developed analytical model to find the necessary conditions that will satisfy the stability requirements and to study how variations in PV array generation, load, and battery regulation affect the voltage stability of the system. Bifurcation analysis is an analytical tool to understand how variations in system parameters affect the system equilibria and impact qualitative changes in the dynamical behavior of the system [24] and its utility is well established for terrestrial power systems [25], [26], [27]. Finally, the analytical findings are verified and validated using an experimental hardware setup.

The model developed in this paper and the associated analyses are well suited for spacecraft power systems featuring distributed energy storage and their reliability requirements consistent with the unique operating conditions that deep space travel vehicles may experience and the specific design requirements and constraints for this class of applications. The findings of this paper facilitate the identification and prediction of vulnerabilities of DC microgrids on board these

specialized vehicles resulting from voltage instabilities that could be expected under system operating conditions. The results presented here aim to set a basis for the design of autonomous power management systems and for the development of preventative control strategies to avoid electrical blackouts due to overloading, improper battery management, distribution network faults, and poor system design.

The remainder of this paper is organized as follows; Section II discusses the special considerations needed for modern spacecraft EPS. Section III develops the model used to analyze the stability. Section IV defines the stability criteria and operational limits for spacecraft EPS control. Section V describes the hardware test procedure and experimental results. Section VI provides conclusions and remarks about the strengths and limitations of the approach, as well as areas for future work.

II. MICROGRID DESIGN CONSIDERATION IN MODERN SPACECRAFT FOR DEEP SPACE EXPLORATION

The designs for DC microgrids on board spacecraft include photovoltaic (PV) power generation, a variety of different power consuming devices including resistive, constant power, and AC loads, distributed energy storage devices that are interconnected via the distribution system, and converters and inverters that interface devices to the power system and are equipped with protective relays and voltage regulators. The operation of the microgrid on board spacecraft shares many similarities with terrestrial microgrids installed on the surface of Earth, but there are a few notable differences that are worth mentioning for modeling and operational considerations. In both instances, a core principle of system management and real-time operation is to maintain the delicate balance between generation and load demand under continuously evolving operating conditions, faults, and disturbances. Such events, regardless of their origin, may initiate transients in critical state variables, such as bus voltages, line currents, power sharing, etc., which if mismanaged can result in exceeding the safe operating limits of the system, ultimately resulting in energy delivery interruptions. The management system for a DC microgrid design for space applications is very similar to the energy management systems (EMS) and distribution management systems (DMS) used in terrestrial power systems.

The automation systems include a supervisory control and data acquisition systems (very similar to the SCADA system that is used in terrestrial power systems but on a much smaller scale) and a set of real-time and off-line power system applications. Given the wide range of spatial-temporal dynamics for the automation and control functions, a wide range of power applications are continuously operated by a combination of control platforms on board the spacecraft and on ground control center that are connected via quasi-real-time communications. Fig. 1 portrays the conceptual structure of a microgrid on board modern spacecraft and its management scheme. There exist a few distinguishing features that separate terrestrial microgrids from spacecraft microgrids. First,

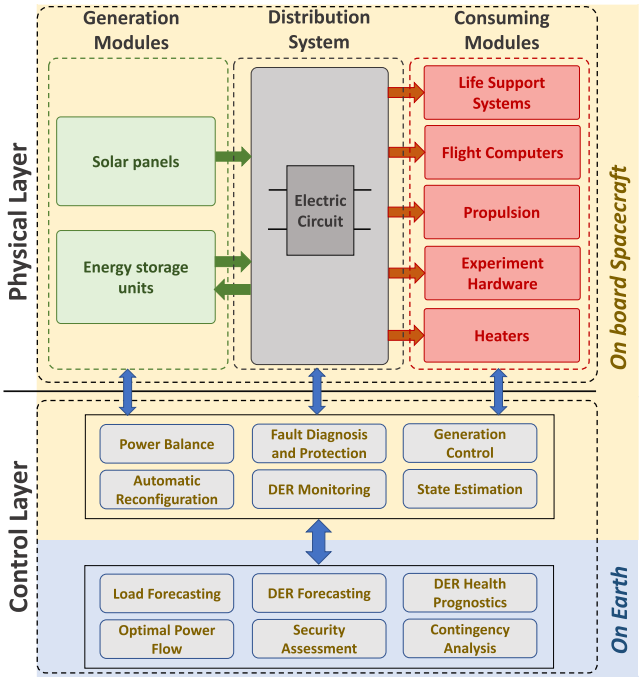

FIGURE 1. The DC microgrid for a spacecraft, its energy management system, and its constitutive components; online analyses run on the computer on board spacecraft and offline analyses run on the computers in control center on Earth.

the electric power grid on board spacecraft is much smaller in scale and more geographically contained than terrestrial grids. Because of these characteristics, it is more feasible to manage the complexity of the spacecraft microgrid in an efficient manner. In addition, data and information flow are essential for autonomous operation, and the structure of the on board spacecraft power system makes it viable to provide the necessary control and communication redundancy and integrated decision-making mechanisms that are required. Second, the degree of uncertainty in the operation of power systems on board spacecraft will be reduced when compared to terrestrial power systems, given that many of its operational scenarios and loads are scheduled and, therefore, offer improved predictability. Additionally, this reduction in uncertainty in its operation enhances the opportunity to mitigate the propagation of interruptions that may occur in the system through the development and implementation of automatic detection, diagnostic and restoration operations. Third, the DC architecture of on board spacecraft power networks, by virtue of the intrinsic operational advantages of DC systems including the time-scales of operation (given the lunar day and night phases), make it computationally feasible to solve both convex and non-convex optimization problems (involving continuous and discrete variables) for security-constrained optimal power flow, state-estimation, and dynamic security assessment. Fourth, energy storage units are highly distributed across the DC power system on board spacecraft which is the core distinguishing architectural element between the of DC microgrids commonly found in terrestrial application and those found in modern space applications. Spacecraft designed for deep space exploration

have reliability requirements significantly higher than those based on earth. The distribution of batteries to provide fault tolerance to all critical spacecraft loads is necessary to meet such requirements. In addition, the health and longevity of batteries are also highly sought after due to the difficulty to repair or replace batteries in space. Therefore, supervisory controls to charge and discharge batteries evenly is used to extend the life of each battery storage device.

The main design challenge lies on the interactions between the load and source subsystems that will impact power quality and potentially cause instabilities, momentary blackouts, malfunctions, and premature failures [20]. Particularly, in spacecraft DC microgrids, available generation and expected load demand are closely matched (unlike terrestrial systems that include spinning reserve), making the system more susceptible to instabilities, and understanding the dynamic behavior of such systems is critical to achieving safe and reliable operation. Although backup solar and storage units are situated for redundant operations, their sensitive and critical nature warrants a high degree of assurance and robustness to prevent actions and interruptions or changes in the system generation mix that could potentially cause momentary blackouts, malfunctions, increasing the potential for system-wide failures.

There are four notable operational factors to consider in the design of microgrids for operation on board modern spacecraft that can challenge the stability of the system. First, as vehicles travel into deep space the irradiance available to the PV arrays decreases, limiting the total generating capacity of the system. Current systems lack the ability to reliably estimate PV generating capacity in real-time due to unexpected damage, such as micrometeorites radiation and plasma damage. Todayŝ spacecraft typically rely on PV power generation as their main power generation source, where terrestrial microgrids often rely on coupling to the centralized grid. The increased reliance on PV availability makes the spacecraft power system more vulnerable to instabilities caused by changes in PV performance and efficiency. Hence robust system operation is needed to effectively manage these uncertainties and disturbances. Second, deep space systems rely on distributed energy storage to provide power during eclipse when power from the PV arrays is unavailable. The distributed architecture makes the power system more robust if an electrical fault should occur. Spacecraft are designed to meet very specific power requirements without exceeding mass requirements. Introducing multiple types of energy storage to the spacecraft also introduces additional risk. The energy storage devices used in modern spacecraft are typically lithium-ion batteries. Third, the distributed energy storage (DES) systems must be carefully controlled to regulate the bus voltage for the loads. Typically, DES devices tightly regulate the voltage using a distributed droop control algorithm. Adjustments in load impedance, generation capacity, and degradation and malfunction of devices and interconnected systems cause frequent changes in system stability that are difficult to monitor and manage in real-time. This includes the impact of spacecraft charging-induced electrostatic arc discharge (ESD) on solar arrays and internal components, that can cause cell degradation and damaging secondary arcs, resulting in the outage of critical components [28]. More details on radiation induced effects on power electronics are discussed in [29] and [30]. Fourth, the control of the source and load subsystems may introduce unexpected and undesirable operating conditions (e.g. instabilities) that depend on specific design parameters and implementation. Therefore, a power management system that provides a high degree of reliability, stability, and resiliency is necessary for the development of next generation of modern spacecraft.

Another consideration in the design of a microgrid on board the next generation of spacecraft for the deep space travel applications is that autonomy is the key enabling solution for deep space travel. Since their inception, spacecraft have relied on automation to perform tasks without human supervision. The increased risk posed by deep space missions will require a transition to autonomy, where systems are able to carry out their functions under significant uncertainties and accurately compensate for faults and unanticipated changes in system dynamics and operating conditions. Future deep space missions are expected to require months of autonomous operation in each subsystem to maintain operations during periods when a crew is not present [31], [32]. Two main challenges exist when developing autonomous capability for spacecraft functions. First, travelling in deep space will be associated with a vast range of risks and uncertainties, not only because of very complex and unorthodox operational environments, but also because of the many unknowns about deep space travel. Hence, the capability to make decisions with high confidence under high degrees of risk, unpredictability, and uncertainty is necessary. Second, the perseverance and reliability of the autonomous decision-making and management system is as robust as the weakest element that in engaged in the process, namely computer software and hardware, sensors, and actuators. Therefore, it is essential to make sure that these constituent elements of autonomy are high-quality with low risk of failure or malfunction. In addition, considerations of redundant elements and contingent operations are important.

Due to the high cost of and inability to quickly service spacecraft, it is imperative that the system remains stable with high assurance of continuing to supply critical power system loads at all times, without manual intervention or the requirement of communications with personnel on Earth. Failures in autonomous mission control have been observed on several occasions over the past several years leading to mission interruptions or loss of the vehicle. For example, a lack of autonomous decision-making led to a shutdown in the Dawn spacecraft electric propulsion system where unaccounted for plasma effects caused a safety shutdown based on exceeding a preset limit. Although this phenomenon was well understood and did not impact the function of the spacecraft, it was not originally accounted for in the protection system. As a result, future shutdowns were prevented by modifying

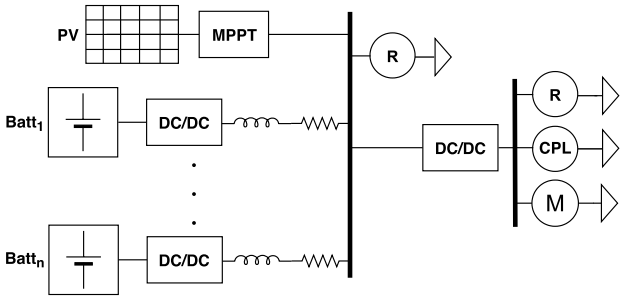

FIGURE 2. Conceptual schematic diagram of DC microgrid for a spacecraft. Batt: battery, PV: photovoltaic array, MPPT: maximum power point tracking, DC/DC: DC-DC converter R: resistive load, CPL: constant power load, M: motor load (AC).

the preset data table threshold [33]. This event highlights the need for more intelligent system awareness and supervision, and the ability of the system to dynamically adjust and adapt to changes in system operating conditions and disturbances.

III. DC ELECTRIC POWER SYSTEM MODEL ONBOARD SPACECRAFT

Modern spacecraft electrical power systems are implemented in modular designs as described in [34] and [35], in the form of a DC microgrid. The main components of the spacecraft electrical power system are loads (AC and DC), distribution network, battery storage, and PV arrays. A conceptual model of a DC power system with source and load subsystems is shown in Fig. 2. Spacecraft power systems often rely on a radial distribution network topology (much like conventional terrestrial AC distribution systems) with some additional redundancies to maintain simplicity and robustness [36]. This allows for simplification in the modeling of the power system. The system stability analysis developed in this paper is directly extendable to remote islanded (grid forming) DC microgrids of a similar topology.

To develop an analytical model of a DC microgrid for a spacecraft electric power system, it is necessary to understand the dynamic behavior of each of the individual components. The components considered here include PV sources controlled by Maximum Power Point Tracking (MPPT), parallel battery systems with droop control, distribution lines, bus capacitance, loads (active, resistive, and inductive) and DC/DC converters. Modeling the behavior of the power source and load subsystems is most important because the interactions between these directly impacts the stability properties of the system.

A. PV ARRAYS AND MAXIMUM POWER POINT TRACKING

PV sources can be connected to the electrical distribution network through a regulating device and the control of that device determines the dynamic response characteristics of the source [37]. For example, PV arrays connected via a DC/DC converter are often controlled via Maximum Power Point Tracking (MPPT), where the objective is to maximize the power output at a given bus voltage. Many algorithms have been developed for MPPT, including the perturb and observe (P&O), hill-climb, and incremental conductance (IncCond) algorithms [38]. These algorithms successfully manage the PV to operate near the maximum power point, unaffected by the behavior of other subsystems. The detailed model of MPPT is not considered in this paper due to the timescale of interest. Hence, the maximum power points (peak of the P-V curves) for each level of solar irradiation are used to model the PV array as a constant power source.

B. BATTERIES AND DROOP CONTROL

The distributed energy storage (battery) systems are responsible for helping to maintain bus voltage within the acceptable operating range. The effects of the other subsystems, such as the PV array and loads, creates challenges for the battery systems to maintain the proper bus voltage. In this study, a droop control method is used for bus voltage regulation as it is the most common method used, though other methods of voltage control schemes can be considered for future studies.

The main objective of droop control is to provide load sharing while accounting for the generating capacity of each source so that no source is overloaded. This paper uses the model for distributed battery systems operating under droop control from [20]. In this model, a battery is connected to the bus through a power converter interface that is modeled as an ideal voltage source with a controlled (virtual) droop resistance, V_i and R_{vi} respectively. The source connects to the system over a distribution line that includes both resistance, R_{li} and inductance L_{li} elements. In general, $R_{vi} \gg R_{li}$, and, thus, it may be assumed that $R_{vi} + R_{li} \approx R_{vi}$.

For n batteries connected in parallel, the reference voltage V_{ref} is set for all sources such that

$$V_{ref} \approx V_1 \approx V_2 \approx \cdots \approx V_n. \tag{1}$$

Due to the similar capacities of the spacecraft energy storage devices, it can be assumed that under normal operating conditions

$$\frac{R_{v_1}}{L_{l_1}} \approx \frac{R_{v_2}}{L_{l_2}} \approx \cdots \approx \frac{R_{v_n}}{L_{l_n}}. \tag{2}$$

Therefore a single term, $\frac{R_d}{L_d}$, can be used to represent the approximate equivalent droop resistance and inductance by taking the average of each of the source parameters

$$\frac{R_d}{L_d} = \frac{1}{n}\sum_{j=1}^{n} \frac{R_{v_j}}{L_{l_j}}. \tag{3}$$

This approximation helps reduce the system of n differential equations into a single differential equation, and the equivalent approximate model simplifies the stability analysis and increases the computational efficiency with minimal impact on accuracy. This approximation may not be valid for microgrids with highly diverse energy storage elements in terms of capacity and storage type, i.e. terrestrial systems.

For a single droop-controlled source j, the dynamics can be modeled using the differential equation

$$\frac{di_j}{dt} = \frac{1}{L_{l_j}}(V_{ref} - v_{bus}) - \frac{R_{v_j}}{L_{l_j}} i_j. \tag{4}$$

The total current provided by all of the droop-controlled sources is given by

$$i_s \approx i_1 + i_2 + \cdots + i_n. \tag{5}$$

Then, the behavior of the entire microgrid can be modeled as a single differential equation representing the sum of the sources as given by

$$\frac{di_s}{dt} = \frac{1}{L_{eq}}[(V_{ref} - v_{bus}) - R_{eq} i_s] \tag{6}$$

where

$$R_{eq} = R_d \frac{L_{eq}}{L_d} \tag{7}$$

and

$$L_{eq} = \frac{1}{\sum_{j=1}^{n} \frac{1}{L_{l_j}}}. \tag{8}$$

The droop-controlled battery systems can be modeled as a voltage source in series with an inductor and resistor as given in equation (6).

C. CONSTANT POWER LOADS

Constant power loads (CPLs) in the system are modeled as current sinks, where the constant current for each CPL is equal to the CPL power divided by the CPL voltage. A DC/DC converter connects the loads to the main bus to regulate the source subsystem voltage to the CPL voltage. It is assumed that the power input to the converter is approximately equal to the power output. Therefore the DC/DC converter can be modeled as a CPL as long as the input voltage is greater than or equal to the required voltage of the loads V_0. If the input voltage falls below V_0, the converter acts as a passive load. Fig. 3 shows the behavior of the DC/DC converter. In [39] and [40] it is shown that active and passive damping can be useful for controlling the converter output for poorly behaved loads. For simplicity, only the CPL behavior of the converters is considered in our analysis and the behavior of the DC/DC converters is given by

$$i(v) = \frac{P}{v} \tag{9}$$

Other types of spacecraft loads such as motors and pumps require AC power and with tightly regulated control, these loads behave as CPLs [39]. In the case of an electric motor, the angular velocity is controlled by the DC/AC inverter as shown in Fig. 4. Given a linear relationship between speed and torque, a given operating speed corresponds to a single value of torque and because power is equal to the product of the speed and torque, the electric motor can also be appropriately modeled as a constant power load [41].

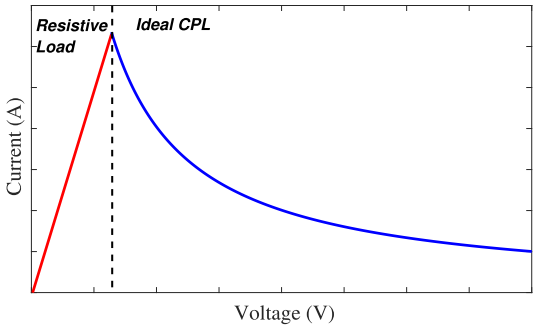

FIGURE 3. Quasi-steady state behavior of the DC/DC converter as a function of the input voltage - this figure displays the resistive load behavior (red line) of the converter when the input voltage is below the minimum converter voltage indicated by the black dashed line. When the input voltage is above the minimum converter voltage it behaves as an ideal CPL as indicated by the blue line.

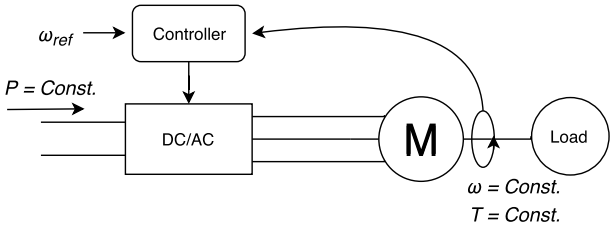

FIGURE 4. DC/AC inverter generating constant power load characteristics.

Lastly, loads with constant impedance tied to the DC bus such as heaters, are modeled simply as resistive loads. These devices do not have the negative impedance characteristics of the CPLs or AC loads and therefore are not a main cause of voltage instability.

IV. STABILITY CRITERIA AND OPERATIONAL CONSTRAINTS

In the previous section, a mathematical model for each subsystem was developed and by integrating them, an approximate model for entire system was developed. In this section, first we derive the necessary conditions for system stability. Then, we describe the inherent limitations for system operation.

A. STABILITY CRITERIA

The integration of the models developed in the previous section produces an approximate model for the entire spacecraft microgrid as shown in Fig. 5. The dynamic equations for the full system are

$$\frac{di_s}{dt} = \frac{1}{L_{eq}}(V_{ref} - v_{bus} - R_{eq} i_s) \tag{10}$$

$$\frac{dv_{bus}}{dt} = \frac{1}{C}(i_s - \frac{v_{bus}}{R} - \frac{P}{v_{bus}}) \tag{11}$$

where the net power P, is defined as the difference between the power consumed and the power generated by the PV arrays:

$$P = P_L - P_{PV}. \tag{12}$$

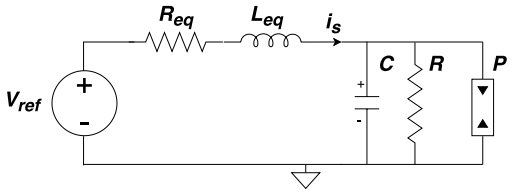

FIGURE 5. Equivalent model for droop controlled DC microgrid.

P represents the amount of power that exceeds the maximum generation capabilities of the PV arrays and must be supplied from the battery systems, and C represents the lumped input capacitances from the DC/DC converters including the capacitor banks that are connected to each bus.

The equilibrium points for this system are determined by setting the right-hand side of the differential equations to zero and then solving for the two fixed points

$$[I_1^*, v_{bus_1}^*] = \left(\frac{V_{ref} - v_{bus_1}^*}{R_{eq}}, \frac{RV_{ref} - a}{2(R_{eq} + R)}\right) \tag{13}$$

$$[I_2^*, v_{bus_2}^*] = \left(\frac{V_{ref} - v_{bus_2}^*}{R_{eq}}, \frac{RV_{ref} + a}{2(R_{eq} + R)}\right) \tag{14}$$

where $a = \sqrt{R^2 V_{ref}^2 - 4PRR_{eq}(R_{eq} + R)}$.

The local (small signal) stability of each fixed point can be determined by evaluating the eigenvalues of the following Jacobian matrix

$$J = \begin{bmatrix} -\frac{R_{eq}}{L_{eq}} & -\frac{1}{L_{eq}} \\ \frac{1}{C} & \frac{1}{C}\left(\frac{P}{v_{bus_i}^{*2}} - \frac{1}{R}\right) \end{bmatrix} \tag{15}$$

The first fixed point, $[I_1^*, v_{bus_1}^*]$ has real eigenvalues with opposite signs resulting in a saddle-node (unstable) equilibrium (fixed) point. The second fixed point, $[I_2^*, v_{bus_2}^*]$ is a stable fixed point when the determinant of J is positive ($\Delta > 0$), and the trace of J is negative ($\tau < 0$). Satisfying both inequalities simultaneously results in a stable system when $C > \frac{L_{eq}}{R_{eq}^2}$. The case where $C \leq \frac{L_{eq}}{R_{eq}^2}$ is discussed in the next section.

The power P satisfies

$$P < \frac{RV_{ref}^2}{4R_{eq}(R_{eq} + R)} = P_{max} \tag{16}$$

where P_{max} is the maximum power that can be provided by the battery system and ensures that the parameter a is real and that a stable solution exists.

The bifurcation diagram, also known as a nose curve, shown in Fig. 6 relates the voltage to the active power and has two branches; (1) the top branch, solid blue line, indicates all stable solutions and (2) the bottom branch, red dashed line, indicates all unstable solutions. The point where the two branches meet is known as the bifurcation point or voltage instability point corresponding to the loading level at which the two solutions coalesce into a single solution [42]. The

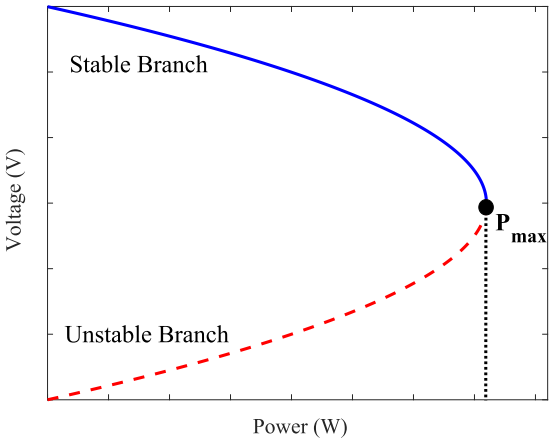

FIGURE 6. Bifurcation diagram of the approximate model.

bifurcation curve reveals the operational limits of the system by indicating the points that must be avoided to prevent instability. For the electric power system considered here, instability occurs when $P > P_{max}$. For example, increasing the CPL, P_L, so that $P_L - P_{PV} > P_{max}$ causes voltage instability that can result in large voltage oscillations and total voltage collapse of the system.

The significance of the bifurcation diagram and analysis is that the system operator (human or computer) can use this information to ensure that the electrical power system is operating within the stable region. Methods such as parameter estimation can be used in conjunction with sensor measurements to accurately approximate the network variables at any point during a mission, then using the stability framework, decisions could be made as to how close the system is to a point of instability. Periodic updates of stability margins are highly beneficial to the power system controller to prevent overloading and other causes of voltage instability and collapse.

B. OPERATIONAL CONSTRAINTS

The operational constraints and critical boundaries for stable and safe management of space-based electrical systems can generally be divided into three main categories. The first category is control limits, which refer to the restrictions imposed by the performance of power regulating devices and control software that commands the electrical system. For example, the droop gain on the distributed energy storage devices must be set such that the power system stays within the voltage limits and produces stable and reliable power. The second category is electrical limits, which pertain to the physical limits that the system must abide by, including generation capability, power transfer limits of distribution feeders, switches, and insulators, and effective system capacitance and inductance. These limits are mainly taken into consideration during the design process and often are compensated by additional physical redundancy to improve the operational security margins of the system. The third category is environmental limits, which pertain to the conditions and the impacts that the

environment, e.g. the vacuum of space, has on the overall performance of the systems, which is well beyond the scope of this paper. Though, the most common environmental limits are secondary impacts such as plasma charging that can cause the solar cells to fail, undesired switching in power electronics, or errors in flight computers. Therefore, manifesting themselves can be considered as special cases of electrical or control limitations.

The three categories listed above manifest themselves in a variety of effects on the behavior of the power system. While there are several conditions that could contribute to voltage instability, this paper examines four probable scenarios that impact power system design for deep space missions. The first condition is the inability to monitor changes in PV generation. Because the spacecraft load and generation are closely matched, there must be extra caution taken to not overload the system. As the PV cells are exposed to the environment of space, degradation is expected to occur making power system planning more difficult. The second condition is the distributed energy storage state during an eclipse. Unlike terrestrial microgrids that may receive auxiliary support from nuclear, fossil fuel-based, or wind resources, a distributed network of batteries are responsible for powering the entire spacecraft during the eclipse periods. The third condition is the use of droop control to dynamically manage distributed energy storage in space systems. This plays a critical role to ensure effective load sharing and that the available energy is utilized optimally. The fourth condition is when the source and load subsystems create an undesirable interaction. In spacecraft, the large numbers CPLs creates negative impedance leading to an unstable condition that is somewhat unique to space systems; although certain terrestrial applications of DC microgrids, such as manufacturing plants may experience similar conditions.

In the following section experiments are performed to test the limits of voltage stability related to the operational factors mentioned above, for each of the probable conditions. This will provide insight into the model's ability to predict the safe operating region of the power system and maintain spacecraft reliability when subject to these credible contingencies.

V. HARDWARE EXPERIMENTATION AND RESULTS

In this section, the results from hardware experiments are used to demonstrate and validate the accuracy and applicability of the analytical model developed in this work. The hardware testbed used here is a laboratory-scale, low voltage system designed to facilitate experimentation with a flexible platform for testing power system control on physical hardware with the capability of testing DC systems. A complete description of the system including the topology, generation units, loads, and its controllers are available in [43] and [44].

To reduce the complexity of the setup and minimize the number of external variables, a single battery source feeding a constant power load was used to simulate an aggregate model of the electrical power system. The testbed uses a 12V, 2A battery that powers a droop-controlled boost converter

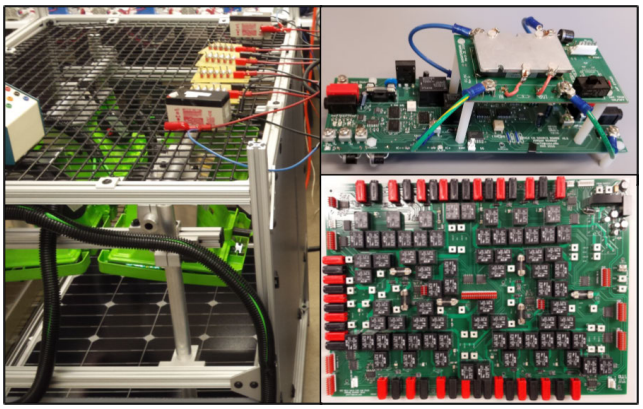

FIGURE 7. Main components of the DC Microgrid Testbed. PV sources, battery energy storage and resistive load banks (left). Bidirectional buck-boost converter module (top right), microgrid power distribution board (bottom right).

with equivalent droop resistance set to $R_{eq} = 5\Omega$ and a reference voltage, $V_{ref} = 12V$. The distribution network consists of a series of bus switches and short transmission lines (<1 meter), with a total measured bus resistance of $R = 106\Omega$. To capture the behavior of the load subsystem, a buck/boost converter is used to provide constant output power that feeds a bank of resistors. The buck/boost converter has a minimum input voltage requirement of 3V, and therefore should not interrupt the behavior before the bifurcation point occurs. The load at the output of the converter is manually controlled. For verification purposes, an analytical model of the system was also developed using the hardware parameters to simulate the voltage behavior. Fig. 7 shows some of the main components of the hardware testbed including energy storage, load banks, power distribution board, and DC converter modules.

To test the mechanisms of voltage instability, the load demand was manually incremented until instability was observed. Here, four experiments were performed and compared with the simulation results. The first three tests were performed such that the system satisfies $C > \frac{L_{eq}}{R_{eq}^2}$ where only the saddle-node bifurcation is present. The final test investigated the presence of a Hopf bifurcation when $C \leq \frac{L_{eq}}{R_{eq}^2}$. The results from each experiment are presented in the following subsections.

To orient the readers with how to interpret the results and plots shown in this section, we provide a brief description of experimental approach. Each of the following figures includes plots from the base case and the modified case that represent the varying operating conditions and parametric sensitivity and are used to illustrate the correlation between the theoretical bifurcation model of the system and the physical system behavior to verify the efficacy and accuracy of the analytical models. The baseline case is established and then three modified cases for parametric sensitivity analyses follow. In each of the modified cases, a single parameter in the system is manipulated and the results are compared to the

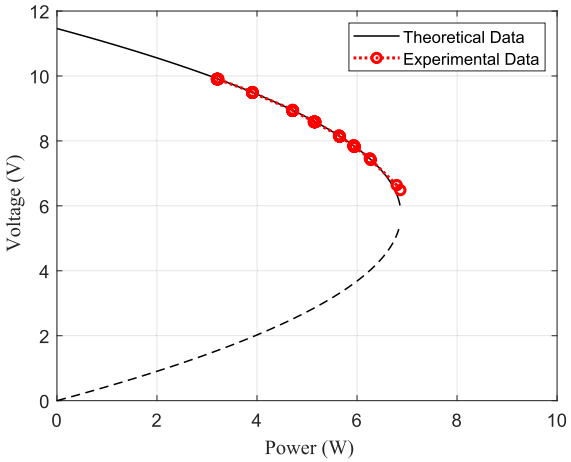

FIGURE 8. Experiment 1: Verification of the analytical model.

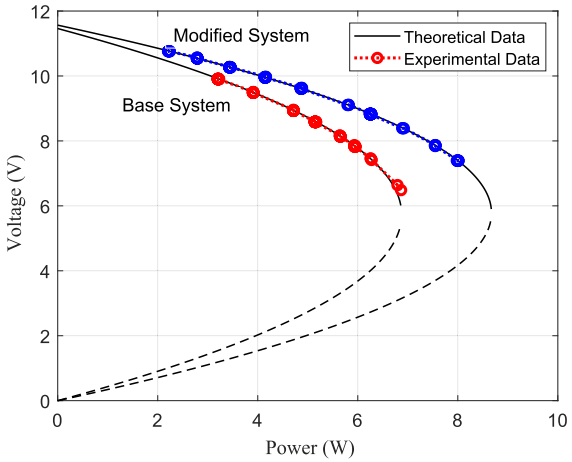

FIGURE 9. Experiment 2: Decrease in equivalent droop resistance.

baseline experiment. In both the base and the modified cases, the bottom dashed branch indicates the theoretically unstable solutions that cannot be realized in practice whereas the top solid line indicates the stable solutions that are verified by experimental measurement data shown with a circled line. The experimental measurement data from the base case are shown in red and the data from the modified case are shown in blue.

A. VERIFICATION OF THE ANALYTICAL MODEL

The first experiment is aimed to verify the analytical model. For this test, the equivalent droop coefficient was set to $R_{eq} = 5\Omega$. The initial load power was set to $P < 2W$ and increased in small steps until the load could no longer be supported by the source. Fig. 8 shows the results from both the analytical calculations and the steady state results from the experimental tests. The bifurcation points of the theoretical model and the experimental measurement data match each other within experimental accuracy. When the bifurcation point is reached, the testbed experiences a sudden oscillation in power coupled with a drop in voltage until the hardware protection limits the power to its final steady state value. The observed oscillations are because the eigenvalues of the system Jacobian are located on the imaginary axis.

The results of this experiment show that the data captured in the analytical model are in good agreement with the behavior observed in the actual hardware testbed and provides verification of the analytical model. The fixed points of the experimental data match with the theoretical predictions and after each increase in load, the power system deviates from the bifurcation curve (transient) and then converges to the new fixed point as determined by the analytical model.

B. EFFECT OF CHANGES IN EQUIVALENT DROOP RESISTANCE

The second experiment addresses the impact of changes in equivalent droop resistance on the system response. The equivalent droop resistance is an estimate of the sum of virtual droop resistances used to control each battery as defined in equation (7). In this experiment, the virtual droop resistance was decreased to $R_{eq} = 4\Omega$ with the remaining parameters set exactly the same as in the first experiment for consistency, and then the load was manually incremented until the source subsystem could no longer meet the load demand and the hardware protection system then takes over. This determines when the system has reached its stability limit. Fig. 9 shows the comparison between experiments 1 and 2. Notice that the bifurcation curve changes shape in a manner consistent with the predicted behavior from the analytical model. The results here suggest that decreasing R_{eq} caused the bifurcation curve to stretch laterally, increasing the amount of constant power load that can be supported (without instability) to about $P = 8.6W$.

Next, the equivalent droop resistance was increased to $R_{eq} = 6.66\Omega$ ($R_{eq} = 5\Omega$ in the first experiment) with all other parameters unchanged. The test results from both values of R_{eq}, displayed in Fig. 10, show that the bifurcation curve becomes shortened, and the system is only able to support a maximum load of $P = 5.1W$. Once again, the experimental data matches closely with the expected theoretical behavior from the analytical model.

C. EFFECT OF CHANGES IN BUS RESISTANCE

The third experiment examined the effect of changes in bus resistance on voltage stability. Bus resistance, R, refers to the total resistance between the positive pole of the distribution system and ground, including the resistive loads that are tied directly to the distribution busbar as well as other residual impedances between the pole and ground. The equivalent droop resistance was set to $R_{eq} = 5\Omega$ as in the first experiment and then the bus resistance is decreased from $R = 106\Omega$ in the first experiment to $R = 57\Omega$. Under these conditions, the condition $R \gg R_{eq}$ is no longer satisfied and we expect a shift in the bifurcation curve as explained in [45].

This experiment was conducted in a manner consistent with the previous experiments, where the load was manually incremented until the systems behavior reflected a sharp

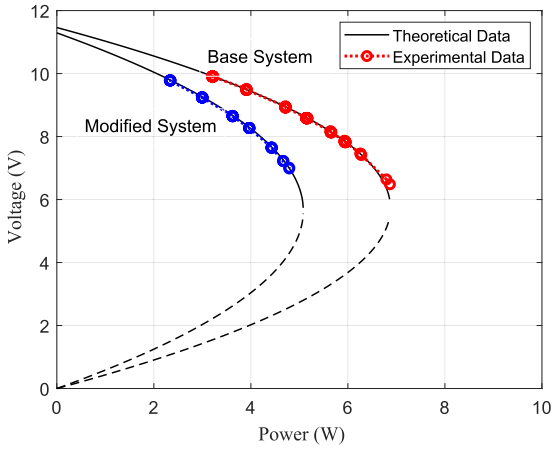

FIGURE 10. Experiment 3: Increase in equivalent droop resistance.

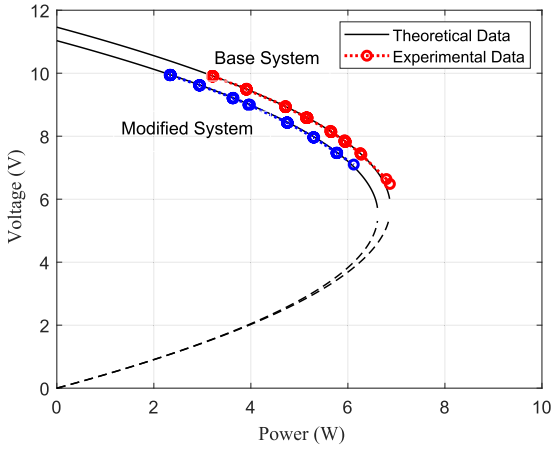

FIGURE 11. Experiment 4: Decrease in bus resistance.

decrease in voltage in conjunction with a sudden spike in current until the hardware protection takes action, indicating that the power system had reached its stability limit. The testbed results for both values of R are shown in Fig. 11. As expected, the theoretical bifurcation curve is shifted downward, and the experimental results confirm the changes as predicted by the analytical model.

D. EFFECT OF CHANGES IN CAPACITANCE, INDUCTANCE, AND EQUIVALENT RESISTANCE

The fourth experiment was an investigation of the relationship between capacitance, inductance, and equivalent resistance. In DC circuits, capacitance has a damping-like effect to mitigate the impact of voltage fluctuations on the circuit by dynamically resisting changes in the bus voltage. Additionally, the inductance affects the rate of change of current in the circuit, and the droop resistance controls the rate of power release in the energy storage devices. Given the total DC power is a product of voltage and current and, therefore, the relationship between R, L, and C is important and inherently dictates the voltage stability during large signal disturbances.

In the previous experiments $C > \frac{L_{eq}}{R_{eq}^2}$ and as detailed in [45], when $C \leq \frac{L_{eq}}{R_{eq}^2}$ a pair of complex conjugate eigenvalues move from the left-half plane toward the

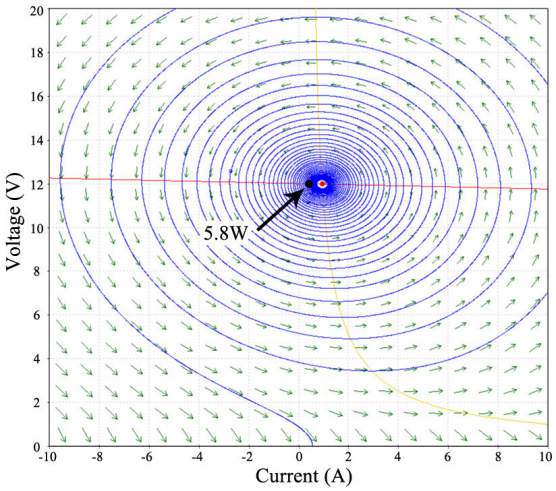

FIGURE 12. Phase portrait of the subcritical Hopf bifurcation - this figure shows the unstable outward trajectory (blue spiral) of the power system operating point from an starting point (red dot) to the right of the subcritical Hopf bifurcation point (black dot).

imaginary axis as the power is increased, generating a Hopf bifurcation. In this experiment the system capacitance is decreased to $C = 238\mu F$, the line inductance is increased to $L = 195\mu H$, and the equivalent droop resistance is set to $R_{eq} = 40\Omega$. All of the remaining parameters are set as described in the previous experiments.

A computer simulation of the hardware testbed suggests that the power at which the Hopf bifurcation will occur is $P = 5.8W$. The analytical methods developed by Guckenheimer and Holmes [46] (pp. 152-156) can be used to prove that the Hopf bifurcation for the system under study is subcritical. Following a subcritical Hopf bifurcation, the trajectories transition to a distant attractor and this can lead to large oscillations and dramatic changes in the system response [47]. Evidence of the subcritical Hopf bifurcation is supported by the computer simulation, where the power was increased to $P = 10W$. From the phase portrait of the dynamical system, the trajectories of the current and voltage near the unstable fixed point can be observed. As shown in Fig. 12, starting from an initial value close to the fixed point, the solution moves in an outward spiral, causing oscillations in voltage and current with increasing amplitude. This analysis suggests the existence of a subcritical Hopf bifurcation.

To conduct this experiment on the hardware testbed, the method of incremental load increase was used, similar to the previous experiments. Fig. 13 displays the results of the experiment as well as the theoretical fixed point. The experimental data matches nicely with the analytical model of the power system in the stable region ($P < 5.8W$). Theoretically, the eigenvalues of the system must exit the stable region when $P \geq 5.8W$, interestingly in the experimental data no unstable or oscillatory behavior is observed. The data continues to match up with the unstable fixed points predicted in the analytical model and the power was increased to $P = 36W$. We suggest these experimental observations are due to the robust regulation of battery storage units that continues to

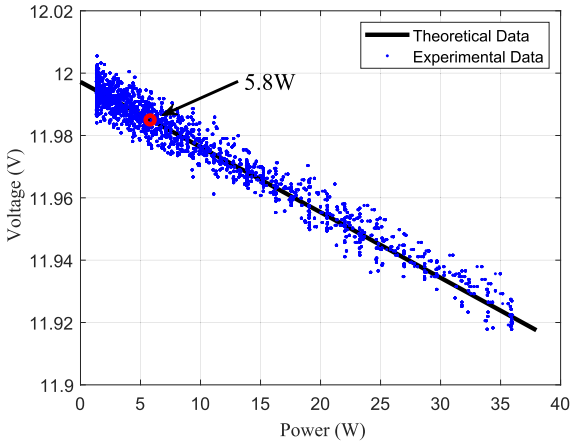

FIGURE 13. **Experiment 5: Increase in inductance and decrease in capacitance.**

provide support and prevent instability. Our findings here stand in contrast to the theoretical analysis derived from the approximate model and the suggested knowledge in the previous literature.

VI. CONCLUSION

This paper discussed the modeling and voltage stability analysis of distributed spacecraft DC power systems. The relationship to terrestrial DC microgrids is presented and differences are discussed. An approximate model for a DC spacecraft power system was presented and bifurcation analysis was used to predict the mechanisms of voltage stability. Last, hardware experiments were used to validate the behavior of the model.

The results of the study provide preliminary validation of the approximate model and its ability to predict conditions that would lead to voltage collapse. The study also suggests that the Hopf bifurcation suggested by the theory and the literature was not reproducible in the experimental data due to the high frequency control of the power electronics. Further work is required to develop a real-time algorithm designed for on board spacecraft stability monitoring. Conducting tests like the ones presented in this paper on space rated hardware with multiple battery sources are needed as a next step. Also, work is needed in the development of the algorithms to estimate the state of the power system including predicted PV output and system capacitance, as these values will change over the course of the mission.

REFERENCES

[1] E. B. Gietl, E. W. Gholdston, B. A. Manners, and R. A. Delventhal, "The electric power system of the international space station—A platform for power technology development," in *Proc. IEEE Aerosp. Conf.*, vol. 4, Mar. 2000, pp. 47–54.

[2] D. T. Ton and M. A. Smith, "The U.S. department of energy's microgrid initiative," *Electr. J.*, vol. 25, no. 8, pp. 84–94, 2012.

[3] B. Lasseter, "Microgrids [distributed power generation]," in *Proc. IEEE Power Eng. Soc. Winter Meeting Conf.*, vol. 1, Jan./Feb. 2001, pp. 146–149.

[4] N. Hatziargyriou, H. Asano, R. Iravani, and C. Marnay, "Microgrids," *IEEE Power Energy Mag.*, vol. 5, no. 4, pp. 78–94, Jul./Aug. 2007.

[5] B. Kroposki, R. Lasseter, T. Ise, S. Morozumi, S. Papathanassiou, and N. Hatziargyriou, "Making microgrids work," *IEEE Power Energy Mag.*, vol. 6, no. 3, pp. 40–53, May/Jun. 2008.

[6] R. Majumder, "Some aspects of stability in microgrids," *IEEE Trans. Power Syst.*, vol. 28, no. 3, pp. 3243–3252, Aug. 2013.

[7] J. Sun, W. Lin, M. Hong, and K. A. Loparo, "Voltage regulation of DC-microgrid with PV and battery," *IEEE Trans. Smart Grid*, vol. 11, no. 6, pp. 4662–4675, Nov. 2020.

[8] F. Gao, R. Kang, J. Cao, and T. Yang, "Primary and secondary control in DC microgrids: A review," *J. Mod. Power Syst. Clean Energy*, vol. 7, no. 2, pp. 227–242, 2019.

[9] J. Frank, L. Spirkovska, R. McCann, L. Wang, K. Pohlkamp, and L. Morin, "Autonomous mission operations," in *Proc. IEEE Aerosp. Conf.*, Mar. 2013, pp. 1–20.

[10] D. Harel, A. Marron, and J. Sifakis, "Autonomics: In search of a foundation for next-generation autonomous systems," *Proc. Nat. Acad. Sci. USA*, vol. 117, no. 30, pp. 17491–17498, Jul. 2020.

[11] T. V. Vu, "Distributed robust adaptive droop control for DC microgrids," Electr. Power Syst. Res., Elsevier, Amsterdam, The Netherlands, Tech. Rep. 146, 2016.

[12] M. Ahmed, L. Meegahapola, A. Vahidnia, and M. Datta, "Stability and control aspects of microgrid achitectures—A comprehensive review," *IEEE Access*, vol. 8, pp. 144730–144766, 2020.

[13] A. Lashab, M. Yaqoob, Y. Terriche, J. C. Vasquez, and J. M. Guerrero, "Space microgrids: New concepts on electric power systems for satellites," *IEEE Electrific. Mag.*, vol. 8, no. 4, pp. 8–19, Dec. 2020.

[14] M. Yaqoob, M. Nasir, J. C. Vasquez, and J. M. Guerrero, "Self-directed energy management system for an islanded cube satellite nanogrid," in *Proc. IEEE Aerosp. Conf.*, Mar. 2020, pp. 1–7.

[15] Y. Gui, R. Han, J. M. Guerrero, J. C. Vasquez, B. Wei, and W. Kim, "Large-signal stability improvement of DC–DC converters in DC microgrid," *IEEE Trans. Energy Convers.*, vol. 36, no. 3, pp. 2534–2544, Sep. 2021.

[16] S. Kotra and M. K. Mishra, "Design and stability analysis of DC microgrid with hybrid energy storage system," *IEEE Trans. Sustain. Energy*, vol. 10, no. 3, pp. 1603–1612, Jul. 2019.

[17] F. Chen, R. Burgos, D. Boroyevich, J. C. Vasquez, and J. M. Guerrero, "Investigation of nonlinear droop control in DC power distribution systems: Load sharing, voltage regulation, efficiency, and stability," *IEEE Trans. Power Electron.*, vol. 34, no. 10, pp. 9404–9421, Oct. 2019.

[18] Y. Ma, K. Corzine, A. Maqsood, F. Gao, and K. Wang, "Stability assessment of droop controlled parallel buck converters in zonal ship DC microgrid," in *Proc. IEEE Electr. Ship Technol. Symp. (ESTS)*, Aug. 2019, pp. 268–272.

[19] O. A. Alimi, K. Ouahada, and A. M. Abu-Mahfouz, "A review of machine learning approaches to power system security and stability," *IEEE Access*, vol. 8, pp. 113512–113531, 2020.

[20] A. P. N. Tahim, D. J. Pagano, E. Lenz, and V. Stramosk, "Modeling and stability analysis of islanded DC microgrids under droop control," *IEEE Trans. Power Electron.*, vol. 30, no. 8, pp. 4597–4607, Aug. 2015.

[21] W. Xie, M. Han, W. Cao, J. M. Guerrero, and J. C. Vasquez, "System-level large-signal stability analysis of droop-controlled DC microgrids," *IEEE Trans. Power Electron.*, vol. 36, no. 4, pp. 4224–4236, Apr. 2021.

[22] J. Liu, W. Zhang, and G. Rizzoni, "Robust stability analysis of DC microgrids with constant power loads," *IEEE Trans. Power Syst.*, vol. 33, no. 1, pp. 851–860, Jan. 2018.

[23] N. H. van der Blij, L. M. Ramirez-Elizondo, M. T. J. Spaan, and P. Bauer, "A state-space approach to modelling DC distribution systems," *IEEE Trans. Power Syst.*, vol. 33, no. 1, pp. 943–950, Jan. 2018.

[24] C. C. C. Karaaslanlı, "Bifurcation analysis and its applications," in *Numerical Simulation-From Theory to Industry*. Rijeka, Croatia: InTech, 2012.

[25] N. H. van der Blij, L. M. Ramirez-Elizondo, P. Bauer, and M. T. J. Spaan, "Design guidelines for stable DC distribution systems," in *Proc. IEEE 2nd Int. Conf. DC Microgrids (ICDCM)*, Jun. 2017, pp. 279–284.

[26] J. Schiffer, R. Ortega, A. Astolfi, J. Raisch, and T. Sezi, "Conditions for stability of droop-controlled inverter-based microgrids," *Automatica*, vol. 50, no. 10, pp. 2457–2469, Oct. 2014.

[27] W. Yi and D. J. Hill, "Stability analysis of all inverter-interfaced generation systems," in *Proc. Power Syst. Comput. Conf. (PSCC)*, Jun. 2018, pp. 1–7.

[28] I. Katz, B. Hoang, and K. Toyoda, "Multicomponent plasma expansion model for arc discharges on large-area solar arrays," *J. Spacecraft Rockets*, vol. 59, no. 1, pp. 324–332, Jan. 2022.

[29] H. Liang, X. Xu, Z. Huang, C. Jiang, Y. Lu, A. Yan, T. Ni, Y. Ouyang, and M. Yi, "A methodology for characterization of SET propagation in SRAM-based FPGAs," *IEEE Trans. Nucl. Sci.*, vol. 63, no. 6, pp. 2985–2992, Dec. 2016.

[30] Z. Song, A. Yan, J. Cui, Z. Chen, X. Li, X. Wen, C. Lai, Z. Huang, and H. Liang, "A novel triple-node-upset-tolerant CMOS latch design using single-node-upset-resilient cells," in *Proc. IEEE Int. Test Conf. Asia (ITC-Asia)*, Sep. 2019, pp. 139–144.
[31] T. Fong, "Autonomous systems: NASA capability overview," NASA Tech. Rep. Server, Mountain View, CA, USA, Tech. Rep. ARC-E-DAA-TN62415, 2018.
[32] J. Crusan, J. Bleacher, J. Caram, D. Craig, K. Goodliff, N. Herrmann, E. Mahoney, and M. Smith, "NASA's gateway: An update on progress and plans for extending human presence to cislunar space," in *Proc. IEEE Aerosp. Conf.*, Mar. 2019, pp. 1–19.
[33] J. R. Brophy, C. E. Garner, and S. C. Mikes, "Dawn ion propulsion system: Initial checkout after launch," *J. Propuls. Power*, vol. 25, no. 6, pp. 1189–1202, Nov. 2009.
[34] B. G. Gardner, "Modular standards for space power systems," in *Proc. 70th Int. Astron. Congr. (IAC)*, 2019, pp. 1–25.
[35] R. C. Oeftering and B. G. Gardner, "Modular power standard for space explorations missions," in *Proc. 70th Int. Astron. Congr.*, 2016, pp. 1–15.
[36] A. D. Bintoudi, C. Timplalexis, G. Mendes, J. M. Guerrero, and C. Demoulias, "Design of space microgrid for manned lunar base: Spinning-in terrestrial technologies," in *Proc. Eur. Space Power Conf. (ESPC)*, Sep. 2019, pp. 1–8.
[37] D. Chen, L. Xu, and L. Yao, "DC voltage variation based autonomous control of DC microgrids," *IEEE Trans. Power Del.*, vol. 28, no. 2, pp. 637–648, Apr. 2013.
[38] T. Esram and P. L. Chapman, "Comparison of photovoltaic array maximum power point tracking techniques," *IEEE Trans. Energy Convers.*, vol. 22, no. 2, pp. 439–449, Jun. 2007.
[39] M. K. Al-Nussairi, R. Bayindir, S. Padmanaban, L. Mihet-Popa, and P. Siano, "Constant power loads (CPL) with microgrids: Problem definition, stability analysis and compensation techniques," *Energies*, vol. 10, no. 10, p. 1656, Oct. 2017.
[40] M. Ashourloo, A. Khorsandi, and H. Mokhtari, "Stabilization of DC microgrids with constant-power loads by an active damping method," in *Proc. 4th Annu. Int. Power Electron., Drive Syst. Technol. Conf.*, Feb. 2013, pp. 471–475.
[41] A. Emadi, A. Khaligh, C. H. Rivetta, and G. A. Williamson, "Constant power loads and negative impedance instability in automotive systems: Definition, modeling, stability, and control of power electronic converters and motor drives," *IEEE Trans. Veh. Technol.*, vol. 55, no. 4, pp. 1112–1125, Jul. 2006.
[42] T. J. Overbye, I. Dobson, and C. L. DeMarco, "Q-V curve interpretations of energy measures for voltage security," *IEEE Trans. Power Syst.*, vol. 9, no. 1, pp. 331–340, 1994.
[43] J. M. Murray, A. Sajadi, and K. A. Loparo, "Design and implementation of microgrid lab-scale hardware/software demonstration," in *Proc. 10th Microgrid Symp.*, Tianjin, China, 2014, pp. 1–7.
[44] J. M. Murray, "Design and implementation of a lab-scale microgrid system," Ph.D. dissertation, Dept. Elect., Comput., Syst. Eng., Case Western Reserve Univ., Cleveland, OH, USA, 2019.
[45] M. Carbone, A. Sajadi, and K. Loparo, "Bifurcation analysis of DC electric power systems for deep space exploration spacecraft," in *Proc. IEEE Power Energy Conf. at Illinois (PECI)*, Feb. 2019, pp. 1–7.
[46] J. Guckenheimer and P. Holmes, "Local bifurcations," in *Nonlinear Oscillations, Dynamical Systems, and Bifurcations of Vector Fields*. Berlin, Germany: Springer, 1983, pp. 117–165.
[47] S. H. Strogatz, *Nonlinear Dynamics and Chaos: With Applications to Physics, Biology, Chemistry, and Engineering*. Boca Raton, FL, USA: CRC Press, 2018.

MARC A. CARBONE (Member, IEEE) received the B.S. degree in engineering physics from John Carroll University, Cleveland, OH, USA, in 2014, and the M.S. and Ph.D. degrees in systems and control engineering from Case Western Reserve University, Cleveland, in 2016 and 2021, respectively. Currently, he is a Control Engineer with the Power Management and Distribution Branch, NASA Glenn Research Center, Cleveland. His research interests include model-based fault detection and diagnosis in electrical power systems. His other research interests include modeling and control of electrical power systems, autonomous systems, and state estimation.

AMIRHOSSEIN SAJADI (Senior Member, IEEE) received the Ph.D. degree in systems and control engineering from Case Western Reserve University, Cleveland, OH, USA, in 2016. He is currently a Research Affiliate with the Renewable and Sustainable Energy Institute, University of Colorado Boulder, Boulder, CO, USA. His main research interests include modeling, planning, dynamics, control, and management of large-scale power systems, including renewable sources and microgrids to enhance the stability, security, and resiliency of energy delivery.

JORDAN M. MURRAY received the Ph.D. degree in systems and controls engineering from Case Western Reserve University, Cleveland, OH, USA, in 2019. His dissertation was on the agent-based control of a lab-scale microgrid model. He was a Postdoctoral Fellow with the Cleveland Clinic Foundation, where he studied eye movements using machine learning techniques. Currently, he is an Embedded Software Engineer with Jergens Inc.

JEFFREY T. CSANK received the M.S. degree in electrical engineering from Cleveland State University, in 2007. He is an Electrical Engineer with the Power Management and Distribution Branch, Power Systems Division, NASA Glenn Research Center. He has been leading the advocate for the development of an autonomous power control capability for human deep space exploration vehicles, for the last six years. He is currently concentrating on developing a microgrid for the lunar surface.

KENNETH A. LOPARO (Life Fellow, IEEE) received the Ph.D. degree in systems and control engineering from Case Western Reserve University, Cleveland, OH, USA, in 1977.

He is currently the Arthur L. Parker Professor with the Department of Electrical, Computer and Systems Engineering; and the Faculty Director of the Institute for Smart, Secure and Connected Systems, Case Western Reserve University. His research interests include stability and control of nonlinear and stochastic systems, with applications to large-scale electricity systems, including generation, transmission, and distribution; nonlinear filtering, with applications to monitoring, fault detection, diagnosis, prognosis, and reconfigurable control; and information theory aspects of stochastic and quantized systems, with applications to adaptive and dual control; and the design of distributed autonomous control systems.

Dr. Loparo has held numerous positions in the IEEE Control System Society, including the Chair of the Program Committee of the 2002 IEEE Conference on Decision and Control and the Control System Society Conference Audit and Finance Committees; the Vice Chair of the Program Committee of the 2000 IEEE Conference on Decision and Control; and a member of the CSS Board of Governors, the CSS Conference Editorial Board, and the Technical Activities Board. He is an Associate Editor of IEEE TRANSACTIONS ON AUTOMATIC CONTROL and *IEEE Control Systems Society Magazine* and the Editor of IEEE TRANSACTIONS ON POWER SYSTEMS.